Cytotherapy, 2017; 19: 586–602

International Society for Cellular Therapy
ISCT®

CrossMark

Extracellular superoxide dismutase increased the therapeutic potential of human mesenchymal stromal cells in radiation pulmonary fibrosis

LI WEI[1], JING ZHANG[2], ZAI-LIANG YANG[3] & HUA YOU[4]

[1]*Key Laboratory of Birth Defects and Reproductive Health of National Health and Family Planning Commission, Chongqing Population and Family Planning Science and Technology Research Institute, Chongqing, China,* [2]*Oncology Department, The First Affiliated Hospital of Jinzhou Medical University, Jinzhou, Liaoning Province, China,* [3]*Department of Breast and Thyroid, Chongqing Hospital of Traditional Chinese Medicine, Chongqing, China, and* [4]*Affiliated Hospital of Academy of Military Medical Sciences, Beijing, China*

Abstract

Background aims. Pulmonary fibrosis induced by irradiation is a significant problem of radiotherapy in cancer patients. Extracellular superoxide dismutase (SOD3) is found to be predominantly and highly expressed in the extracellular matrix of lung and plays a pivotal role against oxidative damage. Early administration of mesenchymal stromal cells (MSCs) has been demonstrated to reduce fibrosis of damaged lung. However, injection of MSCs at a later stage would be involved in fibrosis development. The present study aimed to determine whether injection of human umbilical cord–derived MSCs (UC-MSCs) over-expressing SOD3 at the established fibrosis stage would have beneficial effects in a mice model of radiation pulmonary fibrosis. *Methods.* Herein, pulmonary fibrosis in mice was induced using Cobalt-60 (^{60}Co) irradiator with 20 Gy, followed by intravenous injection of UC-MSCs, transduced or not to express SOD3 at 2 h (early delivery) and 60 day (late delivery) post-irradiation, respectively. *Results.* Our results demonstrated that the early administration of UC-MSCs could attenuate the microscopic damage, reduce collagen deposition, inhibit (myo)fibroblast proliferation, reduce inflammatory cell infiltration, protect alveolar type II (AE2) cell injury, prevent oxidative stress and increase antioxidant status, and reduce profibrotic cytokine level in serum. Furthermore, the early treatment with SOD3-infected UC-MSCs resulted in better improvement. However, we failed to observe the therapeutic effects of UC-MSCs, transduced to express SOD3, during established fibrosis. *Conclusion.* Altogether, our results demonstrated that the early treatment with UC-MSCs alone significantly reduced radiation pulmonary fibrosis in mice through paracrine effects, with further improvement by administration of SOD3-infected UC-MSCs, suggesting that SOD3-infected UC-MSCs may be a potential cell-based gene therapy to treat clinical radiation pulmonary fibrosis.

Key Words: *extracellular superoxide dismutase, human umbilical cord–derived mesenchymal stromal cells, oxidative damage, radiation pulmonary fibrosis, reactive oxygen species*

Introduction

Alveolitis/pneumonitis, an acute phase of radiation-induced lung disease, and its subsequent late/chronic manifestation of radiation pulmonary fibrosis (RPF) are common complications of radiotherapy of chest wall or intrathoracic malignancies, radiotherapy prior to bone marrow transplantation or peripheral blood stem cell transplantation and occupational exposures to high levels of radiation resulting from nuclear reactor accidents [1]. Clinical studies showed that among the patients with treatment of radiotherapy for cancers, the incidence of symptomatic radiation-induced pneumonitis ranges from 5% to 15% [2] and may be as high as 43% [2,3].

RPF, which is characterized by inflammatory cell infiltration, fibroblast proliferation and excessive deposition of extracellular matrix (ECM) proteins in lung parenchyma [4], is a chronic, progressive and fatal interstitial pulmonary disease with a poor prognosis, a high mortality rate and ineffective response to available medical therapies [5]. Thus, many innovative strategies for repair of injured lung have been developed and tested in the past decades. Notably, cell therapy has raised and gained special attention as a new alternative to stimulate lung repair [6].

Correspondence: **Hua You**, MD, PhD, Affiliated Hospital of Academy of Military Medical Sciences, Beijing 100071, China. E-mail: youhua307@163.com;
Correspondence: **Zai-Liang Yang**, MD, PhD, Department of Breast and Thyroid, Chongqing Hospital of Traditional Chinese Medicine, Chongqing 400021, China. E-mail: yangzailiang@aliyun.com

(Received 14 October 2016; accepted 16 February 2017)

ISSN 1465-3249
http://dx.doi.org/10.1016/j.jcyt.2017.02.359

Multipotent mesenchymal stromal cells (MSCs) are primitive cells originating from the mesodermal germ layer and are classically described to give rise to connective tissues, skeletal muscle cells and cells of the vascular system [7]. MSCs may exhibit immunosuppressive properties and have been suggested to be "immune-privileged," and thus are protected from rejection, potentially permitting their use in allotransplantation. It seems certain that MSCs have the capacity to localize to injured lung and differentiate into specific cell types [8,9]. Some reports argue that the therapeutic effects of MSCs in lung fibrosis are mainly mediated by paracrine actions, including stimulation of endogenous repair, angiogenesis and arteriogenesis, attenuating remodeling and reducing apoptosis [10]. Recent reports suggest that MSCs may also promote lung repair through activation of endogenous distal lung airway progenitor cell populations [11], and Cx43-dependent alveolar attachment and mitochondrial transfer [12]. Of interest, injection of murine MSCs, but not human MSCs, differentiated into osteosarcomas in the injured lung. Therefore, human MSCs appear to be more feasible and safer than murine MSCs in the treatment for lung injury [13]. Human MSCs [14] and conditioned medium from human MSCs [15] have been demonstrated to reduce fibrosis in the bleomycin-induced pulmonary fibrosis. However, injection of MSCs at later stage after irradiation would be involved in fibrosis development [5,16].

MSCs can be transduced through several transfection or transduction approaches and are also increasingly described as vehicles for delivery of therapeutic genes and proteins [6]. It is well documented that MSCs transfected with angiopoietin-1 resulted in nearly complete reversal of lipopolysaccharides (LPS)-induced increases in lung permeability [17], and transfected with keratinocyte growth factor (KGF) reduced the histological hallmarks of bleomycin-induced fibrosis, induced proliferation of alveolar type II cells and decreased collagen levels within the lungs [18]. Extracellular superoxide dismutase (SOD3) is a principal enzymatic scavenger of the superoxide anion in extracellular spaces. SOD3 is expressed in especially high levels in mammalian lungs where it is bound to the extracellular matrix through a positively charged heparin/matrix-binding domain [19]. Targeted over-expression of human SOD3 in the lungs of mice significantly protects these mice against bleomycin-induced lung injury, whereas enhanced bleomycin-induced pulmonary damage occurs in mice lacking SOD3 [20–22]. It seems that loss of SOD3 may enhance oxidative stress and injury in the bleomycin-induced lung injury model.

In the present study, we hypothesized that the combined delivery of human umbilical cord–derived mesenchymal stromal cells (UC-MSCs) and SOD3 using gene transfer approach at the established fibrosis stage may show potential beneficial effects on RPF. To our knowledge, this is the first study to assess and highlight the combined cell and gene therapy for treatment of RPF.

Methods

Animals

Eight-week-old female C57BL/6 mice were housed according to the guidelines of the United States National Institutes of Health (NIH) and the local committee for the care and use of laboratory animals. The mice were housed five mice per cage prior to irradiation and one mouse per cage after irradiation. The mice were maintained under standard environmental conditions (temperature 22 ± 2°C, humidity 55 ± 5% and 12-h light/12-h dark cycle), fed a normal pellet diet and provided water *ad libitum* in the cages. All of the experimental procedures involving animals and their care were carried out in accordance with the Guide for the Care and Use of Laboratory Animals published by the NIH, and approved by the local committee for animal use. Every effort was made to minimize the number of animals used as well as their suffering.

Isolation, characterization and differentiation of UC-MSCs

UC-MSCs were collected from the human umbilical cord with informed consent of the mother. The collection was performed in accordance with the ethical standards of the local ethics committee. UC-MSCs were successfully isolated from the Wharton's jelly (WJ) of umbilical cords according to described methods in our previous report [23]. Briefly, fresh umbilical cords were collected after obtaining consent from the mothers. The umbilical cords were rinsed in phosphate-buffered saline (PBS) until the cord blood was cleared, and the blood vessels were removed. The remaining WJ tissue was cut into 1–2 mm^3 pieces and placed in six-well plates in the presence of 0.1% collagenase type II (Sigma) in PBS at 37°C for 1 h. Ten percent fetal bovine serum (FBS, Invitrogen) was then added to stop the digestion. The dissociated mesenchymal cells were dispersed in 10% FBS–Dulbecco's Modified Eagle's Medium (DMEM) and further cultured until well-developed colonies of the fibroblast-like cells reached 80% confluence. Then, the cultures were trypsinized with 0.25% trypsin–ethylenediaminetetraacetic acid (EDTA; Invitrogen) and passaged into new flasks for further expansion. The multipotent differentiation capacity of the UC-MSCs was confirmed by their differentiation into adipocytes, chondroblasts and

osteoblasts using oil red O staining (adipocytes), alcian blue staining (chondroblasts) and alkaline phosphatase (osteoblasts), respectively. The surface markers of the UC-MSCs were also examined using flow cytometry.

Construction of the SOD3-enhanced green fluorescence protein adenoviral expression vector

Ad-SOD3-EGFP, an adenoviral vector containing the human SOD3 gene and a nuclear-targeted enhanced green fluorescence protein (EGFP) gene under the control of the cytomegalovirus (CMV) promoter, was constructed in our laboratory. Briefly, the *Homo sapiens* SOD3 gene was synthesized with insert sites (NotI and HindIII) (Sangon) according to the coding sequence in GenBank. Then, the restriction enzyme digestion product of the T vector containing SOD3 and the adenovirus shuttle vector pDC316-mCMV-EGFP was ligated into pDC316-SOD3-EGFP by T4 DNA ligase (TaKaRa). pDC316-SOD3-EGFP was linearized by PmeI, transformed into competent DH-5α cells, amplified, extracted and purified (TaKaRa). pDC316-SOD3-EGFP and pBHGlox△E1, 3Cre were co-transfected into HEK293 cells by Lipofectamine 2000 (Invitrogen) to obtain the adenoviral expression vector Ad-SOD3-EGFP. The retrieved virus DNA was amplified using polymerase chain reaction (PCR), and, after repeated infections, amplifications and purifications, the virus titer of adenovirus Ad-SOD3- EGFP was determined as 1.6×10^{10} IU/mL by the TCID50 method.

Gene transfer into UC-MSCs

UC-MSCs were exposed to the adenoviral expression vector Ad-SOD3-EGFP at different multiplicities of infection (MOIs): 0, 50, 100, 150, 200, 250 and 300. Two hours later, UC-MSCs were transferred to complete culture medium and incubated for 48 h. The SOD3 expression efficiency of infected cells was detected using flow cytometry. The optimal MOI in the following experiments was chosen for both the highest EGFP expression and viability.

Western blot

Total protein was prepared from the optimal MOI infected UC-MSCs in RIPA Lysis Buffer (Beyotime Biotech). After maintaining the samples for 60 min on ice, Pierce BCA protein assay kit (Thermo Fisher Scientific) was used to determine the protein concentration. Equal amounts of proteins from UC-MSCs of each sample were resolved by sodium dodecyl sulfate polyacrylamide gel electrophoresis (SDS-PAGE) on 10% polyacrylamide gels and then electrotransfered to polyvinylidene fluoride (PVDF) membranes (Millipore Corp). After blocking the membranes in 5% non-fat dry milk in Tris-buffered saline with 0.1% Tween 20 (TBST) for 1 h, the membranes were incubated with anti-SOD3 antibody (1:1000 dilution, Sigma) at 4°C overnight. Then, the membranes were washed with TBST three times and incubated with a secondary antibody, which was conjugated to horseradish peroxidase for 1 h at room temperature. Protein bands were detected using an enhanced chemiluminescence kit (Amersham Biosciences) and imaged using a Molecular Imager ChemiDoc XRS system (Bio-Rad). Signals were quantified using densitometric analyses with Gel-Pro analyzer software, and results are expressed as optical density arbitrary units.

Irradiation and UC-MSCs injection

A total of 240 mice were randomly divided into 6 groups (n = 40 each): normal control group (NC), untreated irradiation group (UI), adenoviral vector SOD3 infected UC-MSCs early treatment group (ES), UC-MSCs early treatment group (EU), adenoviral vector SOD3-infected UC-MSCs delayed treatment group (DS) and UC-MSCs delayed treatment group (DU). Each mouse was anesthetized with 3% sodium pentobarbiturate (50 mg/kg) intraperitoneal (i.p.) injection and subsequently irradiated using a Cobalt-60 (^{60}Co) source. A ^{60}Co irradiator (Model GWXJ80, NPIC) was used to conduct gamma ray irradiation, and the mice were irradiated with 20 Gy at a dose rate of approximately 150 cGy/min. The beam was strictly restricted to the entire thorax. Mice in the ES and EU groups were injected with adenoviral vector SOD3-infected UC-MSCs (1×10^6 cells) and UC-MSCs (1×10^6 cells) injections through the tail vein in a 200 μL volume at 2 h post-irradiation. Mice in the DS and DU groups were injected with adenoviral vector SOD3-infected UC-MSCs (1×10^6 cells) and UC-MSCs (1×10^6 cells) injections through the tail vein in a 200 μL volume at 60 days post-irradiation. Mice in the UI group were not provided any treatment after irradiation. Mice in the NC group were fed normally and not irradiated during the same period. The mice were observed daily for up to 120 days post-irradiation.

Specimen processing and histology

Mice in the NC, UI, ES and EU groups were humanely killed at 3, 7, 30, 60, 90 and 120 days after experiment (n = 6 each time point). Mice in the DS and DU groups were humanely killed at 63, 67, 90 and 120 days after experiment (n = 6 each time point). Blood samples were collected from heart, and allowed to clot for 1 h at room temperature. Serum were obtained after centrifugation at 4000 rpm for 10 min at 4°C, and stored at −80°C. The left lungs were fixed with 4% paraformaldehyde for histological and

immunohistochemical analysis. The right lungs were snap frozen with dry ice powder and stored in liquid nitrogen tank until use. The left lungs were then dehydrated in ethanol and embedded in paraffin. Lung sections (5-μm thickness) were deparaffinized, rehydrated and stained with hemotoxylin/eosin (H-E) and Masson's trichrome.

Immunohistochemical analysis

Immunohistochemistry was performed according to a minor modification described in the methods in our previous reports [23–25]. Lung sections (5-μm thickness) were deparaffinized and rehydrated through graded alcohol and following microwave antigen retrieval with citrate buffer (10 mmol/L sodium citrate, pH 6 for 10 minutes). Endogenous peroxidase was quenched using 3% H_2O_2 for 10 min. The sections were incubated with surfactant protein-B (SPB) antibody (1:1000, Millipore), Iba1 antibody (1:1000, Wako), human nuclei antibody (MAB1281, 1:1000, Millipore) or alpha smooth muscle actin (a-SMA) antibody (1:1000, Millipore) at room temperature overnight. The primary antibody was omitted for the negative control. After washing with PBS, the sections were incubated with Polymer Helper for 30 min at room temperature, and subsequently incubated with polyperoxidase-anti- mouse/rabbit immunoglobulin (Ig)G for 30 min at room temperature using the Polink-2 Polymer-HRP Detection System (GBI Labs) according to the manufacturer's protocol. The slides were developed with diaminobenzidine (DAB; DakoCytomation), counterstained with Mayer's hematoxylin, dehydrated with increasing concentrations of alcohol, cleared in xylene and mounted in neutral balsam (Sigma).

Measurement of collagen content in pulmonary

The collagen levels in lung were examined by Hydroxyproline (Hyp) assay according to the manufacturer's standard protocol (Nanjing Jiancheng Bioengineering Institute). Some right lung tissue samples were hydrolyzed in 1 mL lysis buffer solution at 100°C for 20 min. Absorbance of colored products was measured at 550 nm. The Hyp content was expressed as micrograms of Hyp per gram of wet weight (mg/g).

Analysis of lipid peroxidation

Some frozen right lungs were rinsed, weighed and then homogenized in ice-cold saline for 10 min. Homogenates were collected after centrifugation at 4000 rpm for 10 min at 4°C, and supernates were used for the measurement of the total protein, malondialdehyde (MDA) content, total superoxide dismutase (SOD) activity and catalase (CAT) activity biomedical assay. Polyunsaturated lipids are susceptible to an oxidative attack, typically by reactive oxygen species, resulting in a chain reaction with the production of end products such as MDA. We determined lipid peroxidation by quantifying the amount of MDA via the measurement of a red-complex produced during the reaction of thiobarbituric acid (TBA) with MDA. A microplate reader (UV-7504) was used to measure the absorbance of cellular MDA at 532 nm, and the MDA content was calculated according to the detailed instructions of the MDA assay kit (Nanjing Jiancheng Bioengineering Institute).

Enzyme activity assays

Lung samples were collected as described above. In addition, total SOD activity in culture medium at 48 h post-transfection using the optimal MOI was also measured. The activities of two enzymes, SOD and CAT, were determined using commercial kits according to the manufacturer's protocols (Nanjing Jiancheng Bioengineering Institute). Enzyme activity assays were carried out using a UV-visible spectrophotometer (UV-7504).

Cytokine expression in serum

The levels of transforming growth factor-β1 (TGF-β1) and interferon-γ (IFN-γ) in serum were determined using commercially available enzyme-linked immunosorbent assay (ELISA) kits according to the manufacturer's protocols (Boster Biological Technology). The optical density (OD) value was determined by an ELISA reader at a wavelength of 450 nm and calculated in the linear part of the curve.

Morphometric analysis

The semi-quantitative analysis of fibrosis was performed by an independent pathologist, who was blinded to the experimental conditions. Fibrosis score was performed according to a minor modification of the previously described method [15], taking into account both the extent of tissue involvement and the types and severity of changes within affected areas. Fibrosis distribution, collagen deposition (both on Masson's trichrome–stained sections), fibroblast proliferation and alveolar obliteration (both on H-E–stained sections) were used to assess fibrotic degree. Fibrosis distribution was scored as 1, 2, 3 or 4, representing 1%–25%, 26%–50%, 51%–75% or 76%–100% of the area of the whole section affected, respectively. Severity parameters (fibroblast proliferation, collagen deposition and alveolar obliteration) were scored as a value of 0, 1, 2 or 3 for absent, mild, moderate or severe, respectively. Specifically,

fibroblast proliferation evaluates the presence of spindle cells, morphologically indicative of fibroblasts. Collagen deposition evaluates the presence of blue-stained collagen areas, and alveolar obliteration evaluates the amount of area characterized by the thickening of inter-alveolar septa that reduces alveolar spaces. For each animal, one H-E–stained section and one Masson's trichrome–stained section under Olympus microscopy were carefully examined. The fibrosis score for each animal was obtained by taking the sum of the score of the fibrosis severity parameters and multiplying this result by the fibrosis distribution score. For each group, six animals were analyzed, and the mean score of each group was determined as the total score of all sections divided by six. For the immunohistochemical analyses of SPB, α-SMA and Iba1, the number of positive cells was counted in one representative field for each section under 100 × magnification for a total of six fields per group. The total number of positive cells was calculated per animal and the mean was calculated per group. Large airways and lung vessels were excluded for all analysis.

Statistics

All quantitative data are expressed as the mean value ± standard deviation (SD) or standard error of mean (SEM). All statistical analyses were performed using SPSS statistics software. A value of $P < 0.05$ was considered to indicate a statistically significant difference.

Results

SOD3 is highly expressed in infected UC-MSCs under optimal conditions

Forty-eight hours after virus infection, flow cytometry indicated that the efficiency of Ad-SOD3-EGFP infection increased with increasing MOI. However, when the MOI exceeded 200, the infection efficiency no longer increased, and MOI values of 200 or more led to negative effects on cell growth (Figure 1A). Therefore, adenoviral infection was performed with the MOI value of 200 as the optimal condition for infection, green fluorescence was strongly expressed in infected UC-MSCs under the fluorescence microscope (Figure 1B and 1C), SOD3 expression was analyzed using Western blot and total SOD activity in culture medium was examined using a biochemical assay.

In Ad-SOD3-EGFP–infected UC-MSCs, SOD3 expression was 2.5-fold higher than that in uninfected UC-MSCs, and 1.8-fold higher than that in Ad-EGFP–infected UC-MSCs (Figure 1D). The activity of SOD in Ad-SOD3-EGFP–infected UC-MSCs [(21.36 ± 0.94) U/mL] was significantly higher than those in the Ad-EGFP infected UC-MSCs [(5.34 ± 0.90) U/mL] and uninfected UC-MSCs [(4.92 ± 0.19) U/mL] (Figure 1E). These results demonstrated that adenoviral expression vector, Ad-SOD3-EGFP, could effectively infect UC-MSCs and increase SOD3 expression and total SOD activity. However, Ad-EGFP failed to show these effects. Hence, we excluded Ad-EGFP for further experiment.

UC-MSCs survive and engraft in pulmonary

We stained the lung sections with a marker of human nuclei, MAB1281, to identify surviving UC-MSCs. Some UC-MSCs were found in lung sections of UC-MSC–treated animals (Figure 2).

SOD3 further enhances UC-MSC–induced histological improvement in pulmonary

Previous studies have demonstrated that early injection of MSCs may ameliorate the irradiation-induced fibrotic effects, but late delivery of MSCs may contribute to the irradiation-induced fibrotic lesions [5,16]. The aim of the current study was to analyze whether injections of SOD3-infected UC-MSCs at a later stage after irradiation could reduce the damaging effects of irradiation and subsequent fibrosis. The Masson's trichrome staining of lung sections at different time points post-irradiation revealed that collagen deposition was seen from 60 days post-irradiation (Figure 3A). Therefore, SOD3-infected UC-MSCs and UC-MSCs were intravenously injected at 60 days post-irradiation as the later stage according to our observation and previous reports [5,16].

Histological examination of lung sections using H-E and Masson's trichrome staining revealed the typical lung fibrosis features of lung architecture and collagen deposition at 120 days post-irradiation (Figure 3A). Markedly thickened alveolar walls, collapsed alveoli, foam-like cells in the alveolar space, increased exudation, diffuse accumulation of inflammatory cells, marked hyperplasia of parenchymal cells, extensive deposition of collagen and regional fibrosis foci were observed in H-E and Masson's trichrome staining of irradiated pulmonary sections at 120 days post-irradiation. Notably, alveolar hemorrhage was obvious and serious in the UI group and DS- and DU-treated animals (Figure 3B). The pathological alterations in DS- and DU-treated animals were similar as in the irradiation-only animals (UI group) as determined using H-E and Masson's trichrome staining of lung sections at 120 days post-radiation (Figure 3). Of interest, evident fibrosis and alveolar hemorrhage were not observed in ES- and EU-treated animals as determined using Masson's trichrome staining and H-E staining of lung sections, respectively. Pathological observations of the lung

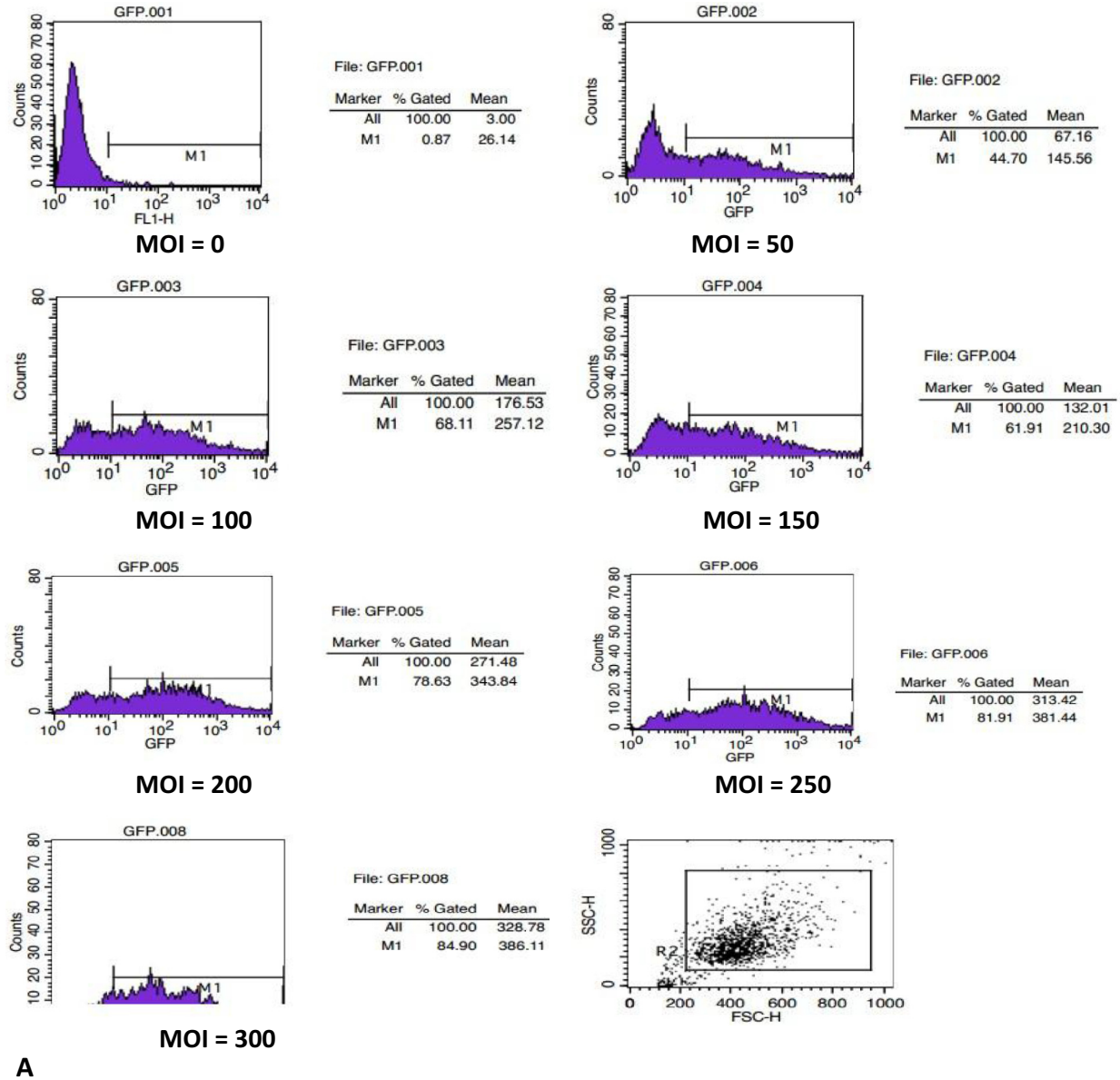

Figure 1. SOD3 was highly expressed in infected UC-MSCs under optimal conditions. (A) The infection efficiency of SOD3-infected UC-MSCs was detected using flow cytometry. Flow cytometry results indicated that the efficiency of SOD3 infection increased with increasing MOI. However, when the MOI exceeded 200, the infection efficiency no longer increased, and MOI values of 200 or more led to negative effects on cell growth. Green fluorescence was strongly expressed in Ad-EGFP–infected UC-MSCs (B) and Ad-SOD3-EGFP–infected UC-MSCs (C) under the fluorescence microscope (MOI = 200). (D) SOD3 expression was analyzed in uninfected control cells, Ad-SOD3-EGFP–infected UC-MSCs and Ad-EGFP–infected UC-MSCs using Western blot. (E) Total SOD activity in culture medium was examined from uninfected control cells, Ad-SOD3-EGFP–infected UC-MSCs and Ad-EGFP–infected UC-MSCs using a biochemical assay. Error bars represent the SD. Double asterisk indicates $P < 0.01$. Abbreviation: n.s., not significant. Scale bar is 100 μm in B and C.

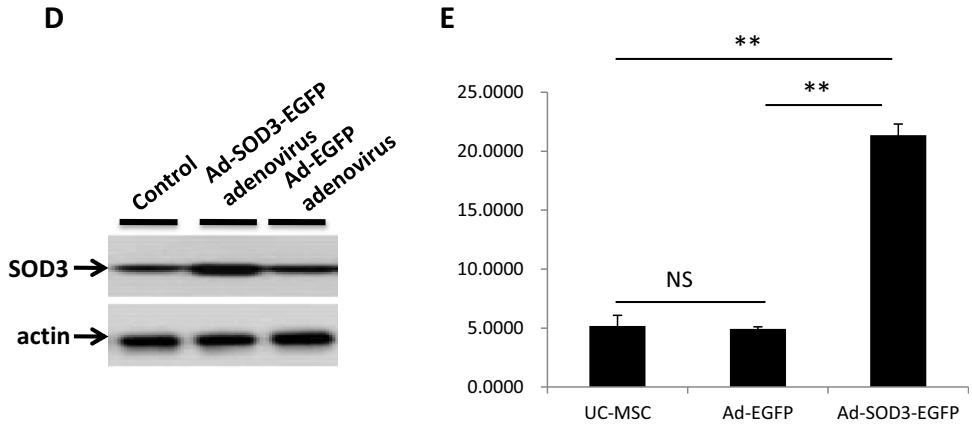

Fig. 1. Continued

tissues using H-E staining further revealed that lung architecture was kept better in the ES-treated animals compared with the EU-treated animals (Figure 3B).

The fibrosis scores in ES- and EU-treated animals were significantly lower than those in DS- and DU-treated animals at 120 days post-irradiation. The fibrosis score in ES-treated animals was significantly lower than that in EU-treated animals at 120 days post-irradiation. However, there was no significant difference in the fibrosis scores among the three groups: UI, DS and DU (Figure 3C). Taken together, these results revealed that early treatment, but not late treatment, significantly attenuated the irradiation-induced lung histological damage *in vivo*. SOD3 further improved the histological damage in pulmonary tissue ameliorated by US-MSCs.

SOD3 further inhibits (myo)fibroblast proliferation, reduces inflammatory cell infiltration and protects alveolar epithelial type II cell damage

The (myo)fibroblast activation and proliferation have been recognized as important contributors to pulmonary fibrosis. Macrophage infiltration has been implicated in the irradiation-induced lung fibrotic process. Alveolar epithelial type II (AE2) cell injury has been considered as both a direct and indirect consequence of irradiation pulmonary damage effects. We subsequently investigated the effects of the early and late delivery of UC-MSCs with or without SOD3 on the (myo)fibroblast, macrophages and AE2 cells, respectively. We used α-SMA antibody, a (myo)fibroblast marker, Iba1 antibody, a macrophages marker and SPB antibody, an AE2 cells marker, to perform immunohistochemical analysis of lung sections.

A very strong expression of α-SMA and Iba1 were seen in the irradiated pulmonary tissue at 120 days post-irradiation (UI group; Figure 4A and 4C). The α-SMA and Iba1 expression in DS- and DU-treated animals was similar to the radiation-only animals at 120 days post-radiation. The ES and EU treatment significantly reduced the α-SMA and Iba1 expression (Figure 4A and 4C). The ES treatment further reduced the α-SMA and Iba1 expression compared with EU treatment (Figure 4A and 4C). In contrast, a weak SPB

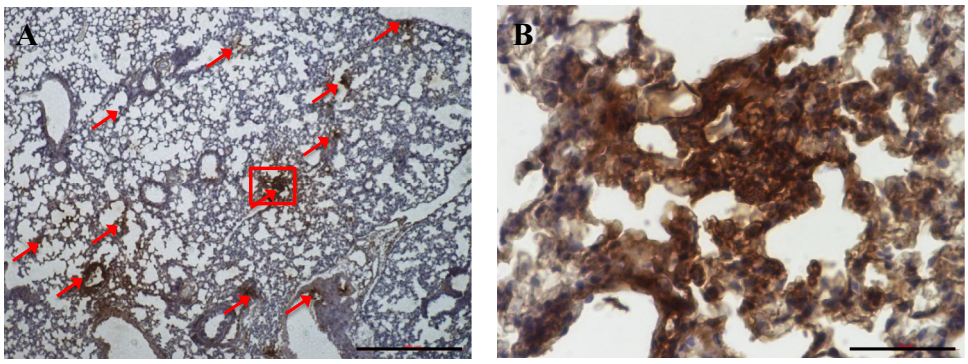

Figure 2. UC-MSCs survived and engrafted in pulmonary. Representative immunohistochemical staining micrographs of a marker of human nuclei, MAB1281, in lung sections from ES treated-animals at 120 days post-irradiation. B is magnified image of boxed area in A. Arrows indicate UC-MSCs. Scale bar is 500 μm in A and 50 μm in B.

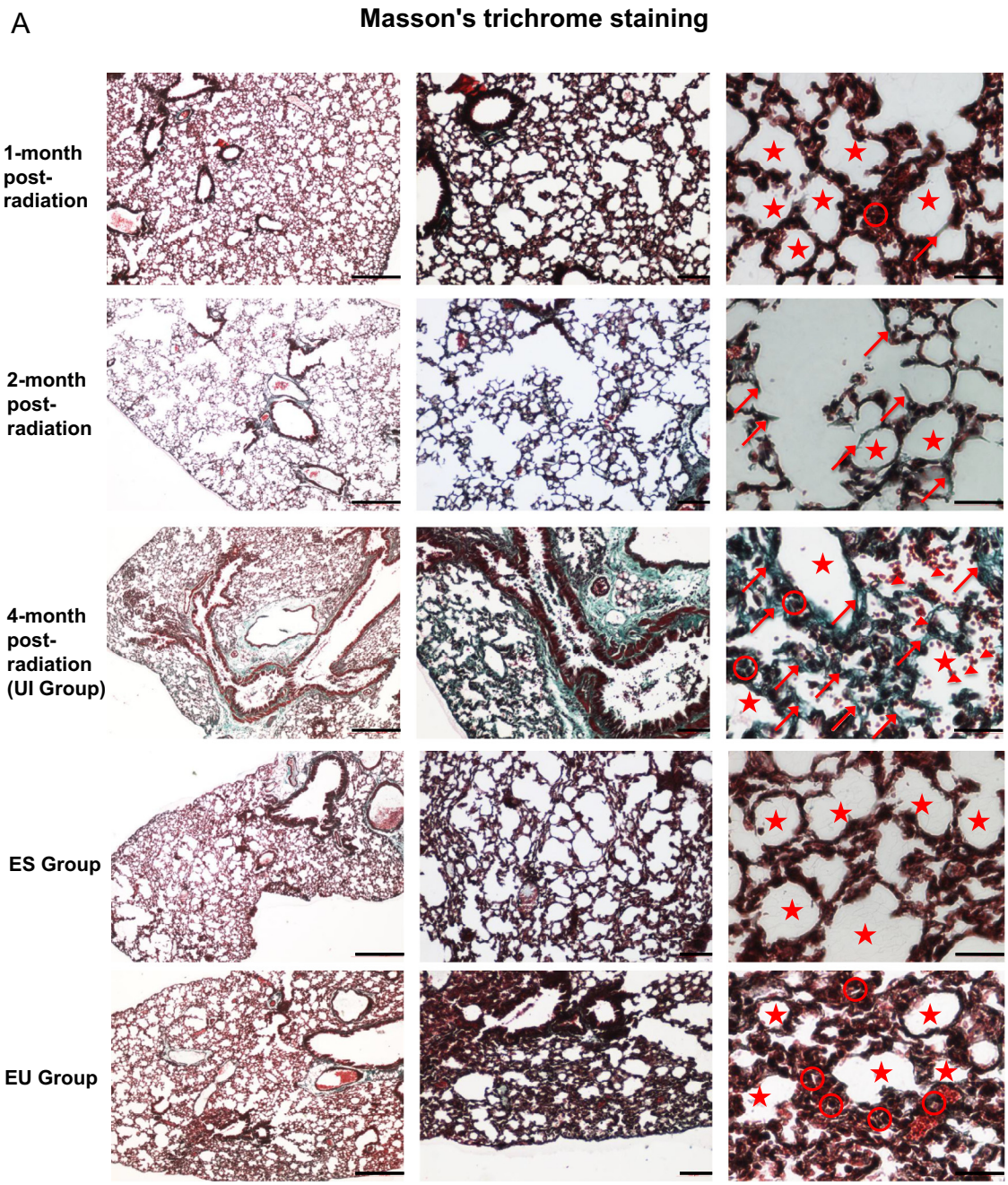

Figure 3. SOD3 further enhanced UC-MSCs and induced histological improvement in pulmonary. (A) Representative micrographs of Masson's trichrome–stained lung sections from 30, 60 and 120 days post-irradiation with a single dose of 20 Gy, ES- and EU treated-animals at 120 days post-irradiation. (B) Representative micrographs of H-E–stained lung sections from normal control, untreated irradiation, early injection of SOD3-infected UC-MSCs and early injection of UC-MSCs. Bars: 500 μm in the left column, 100 μm in the middle column and 50 μm in the right column of A and B. Arrows indicate collagen deposition and increased mucus secretion, hollow circles indicate markedly thickened alveolar walls, five-pointed stars indicate alveolar space and arrowheads indicate alveolar hemorrhage. (C) The semi-quantitative analysis of fibrosis was performed and fibrosis score was obtained taking into account both the extent of tissue involvement and the types and severity of changes within affected areas. Error bars represent the SEM. Single asterisk represents $P < 0.05$ and triple indicates $P < 0.001$. Abbreviations: DS, delayed injection of SOD3 infected UC-MSCs; DU, delayed injection of UC-MSCs; ES, early injection of SOD3 infected UC-MSCs; EU, early injection of UC-MSCs; NC, normal control; n.s., not significant; UI, untreated irradiation.

expression was seen in the irradiated pulmonary tissue at 120 days post-irradiation (UI group; Figure 4B). The SPB expression in DS- and DU-treatment animals was similar to the radiation-only animals at 120 days post-radiation. The ES and EU treatment significantly enhanced the SPB expression (Figure 4B). The ES treatment further enhanced the SPB expression compared with EU treatment (Figure 4B).

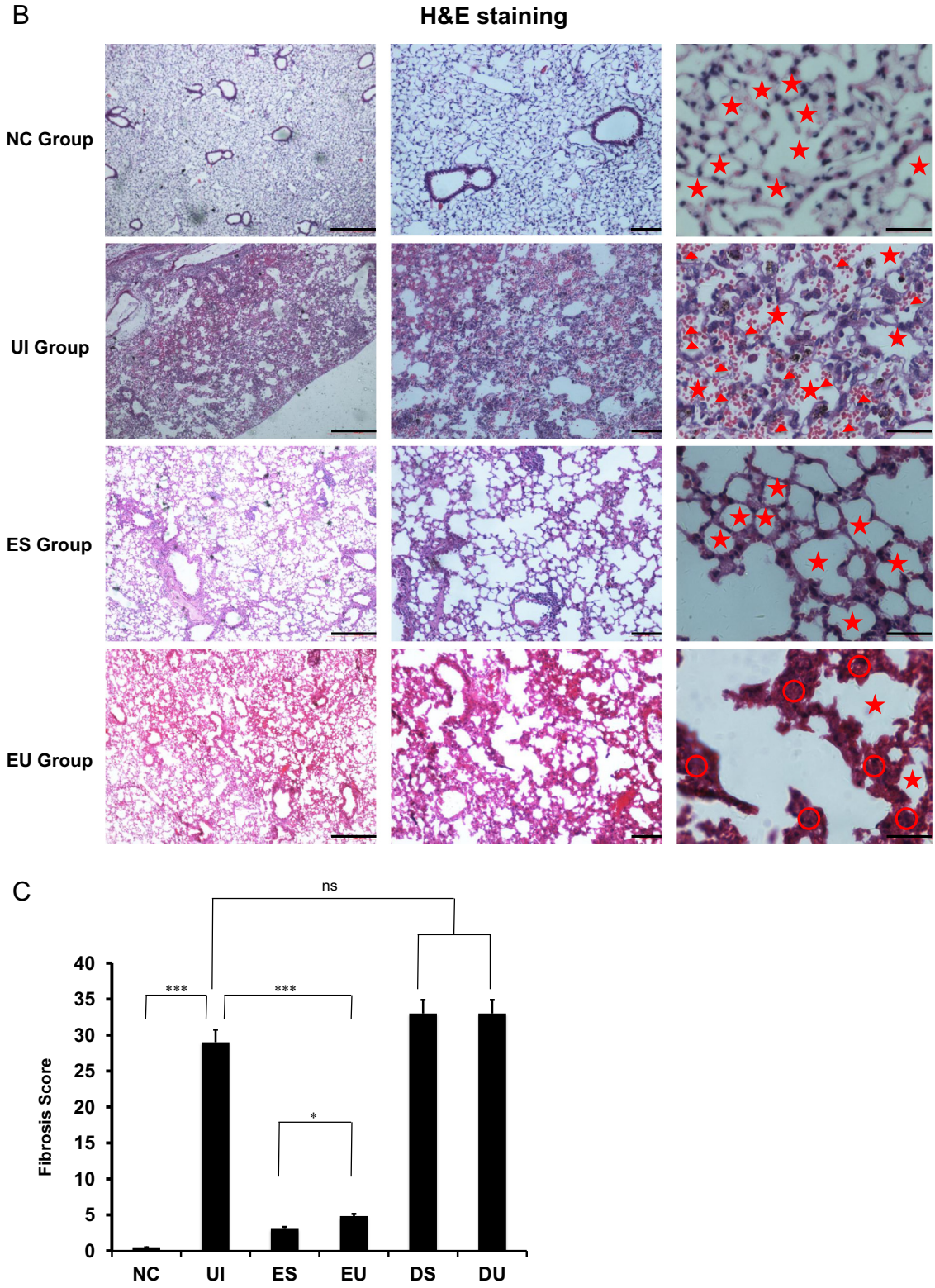

Fig. 3. Continued

The numbers of α-SMA and Iba1 immunohistochemical-positive cells in ES- and EU-treated animals were significantly lower than those in DS- and DU-treated animals at 120 days post-irradiation (Figure 4C). The number of α-SMA and Iba1 immunohistochemical-positive cells in ES-treated animals was significantly lower than that in EU-treated animals at 120 days post-irradiation

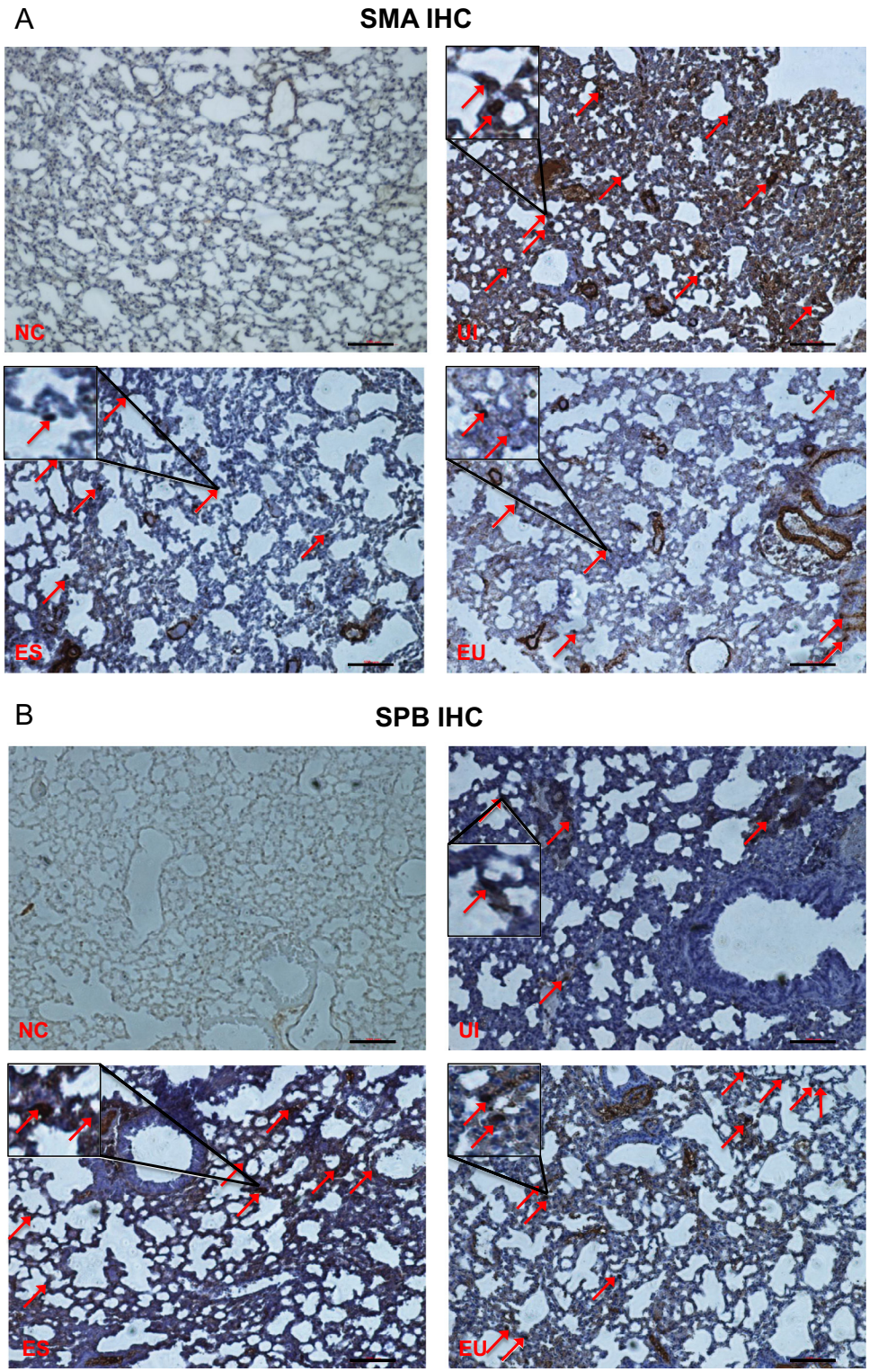

Figure 4. SOD3 further inhibited (myo)fibroblast proliferation, reduced inflammatory cell infiltration and protected AE2 cells damage. Representative micrographs of α-SMA (A), SPB (B) and Iba1 (C) in lung tissues from NC, UI, ES and EU. Bars: 100 μm. (D) The number of α-SMA, SP-B and Iba1 immunohistochemical-positive cells were counted and quantified. Error bars represent the SEM. Single asterisk represents $P < 0.05$, double asterisk indicates $P < 0.01$ and triple indicates $P < 0.001$. Abbreviations: DS, delayed injection of SOD3 infected UC-MSCs; DU, delayed injection of UC-MSCs; ES, early injection of SOD3 infected UC-MSCs; EU, early injection of UC-MSCs; NC, normal control; n.s., not significant; UI, untreated irradiation.

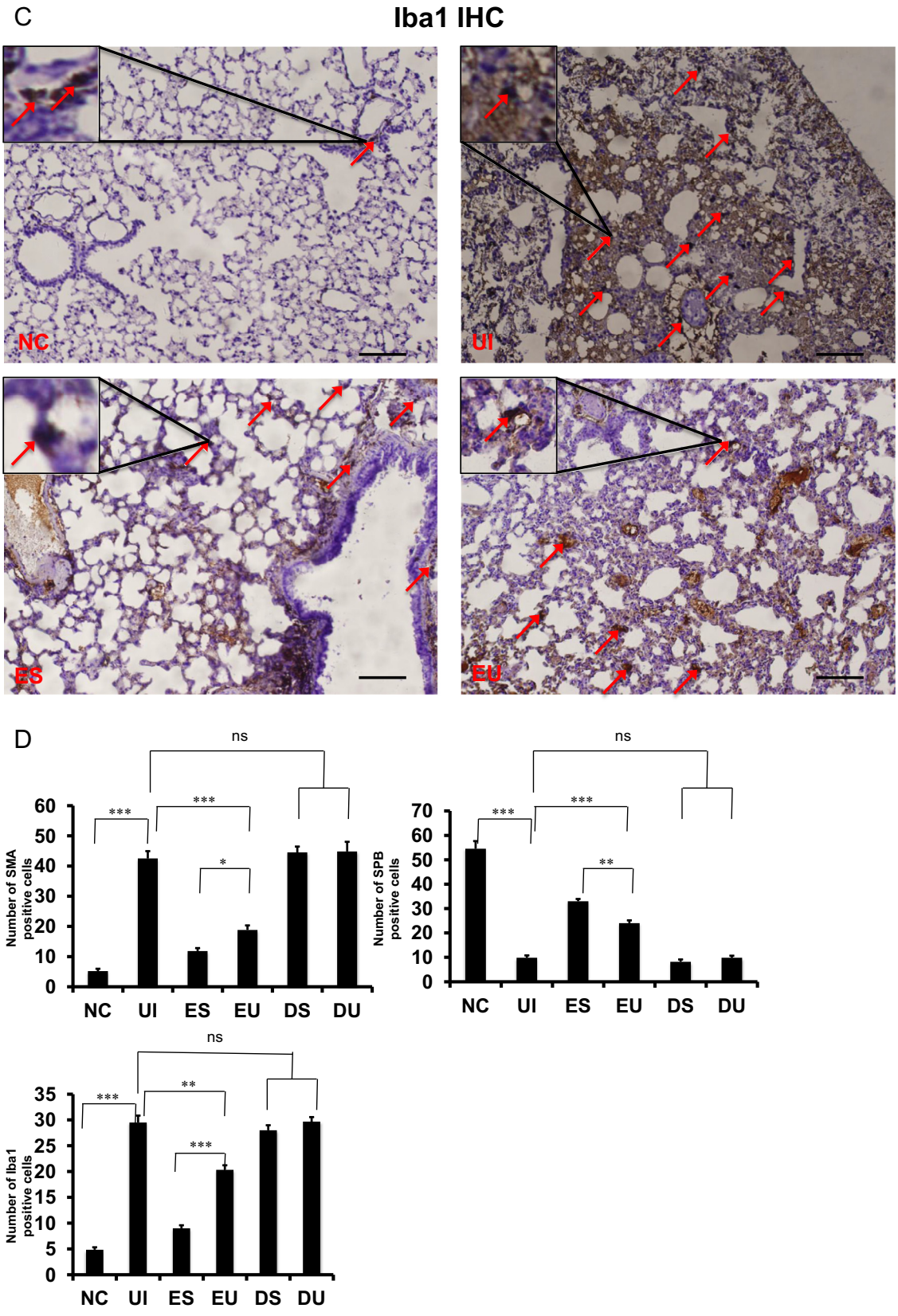

Fig. 4. Continued

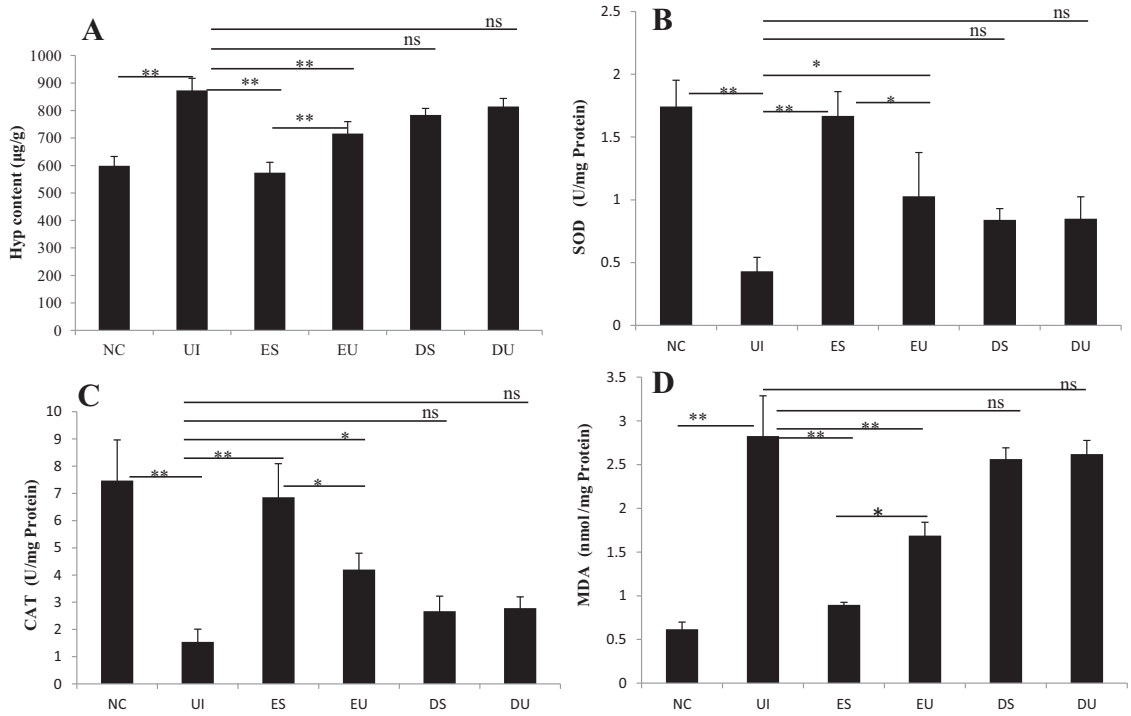

Figure 5. SOD3 reduced collagen levels and restored redox state homeostasis ameliorated by US-MSCs in pulmonary. (A) The Hyp content, as a reliable marker of lung tissue collagen protein level, was measured using a biochemical assay, and presented as micrograms of Hyp per gram of wet weight (mg/g) (n = 6). The total SOD activity (B), CAT activity (C) and MDA content (D) in lung tissues were determined at 120 days post-irradiation (n = 6). Error bars represent SEM. Single asterisk represents $P < 0.05$ and double asterisk indicates $P < 0.01$. Abbreviations: DS, delayed injection of SOD3 infected UC-MSCs; DU, delayed injection of UC-MSCs; ES, early injection of SOD3 infected UCMSCs; EU, early injection of UC-MSCs; NC, normal control; n.s., not significant; UI, untreated irradiation.

(Figure 4C). Conversely, the numbers of SPB immunohistochemical-positive cells in ES- and EU-treated animals were significantly higher than those in DS- and DU-treated animals at 120 days post-irradiation (Figure 4C). The number of SPB immunohistochemical-positive cells in ES-treated animals was significantly higher than that in EU-treated animals at 120 days post-irradiation (Figure 4C). However, there was no significant difference in the number of α-SMA, Iba1 and SPB immunohistochemical-positive cells among the following three groups: UI, DS and DU (Figure 3C).

These results confirmed that the early delivery of UC-MSCs, but not the late delivery, inhibited (myo)fibroblast proliferation, reduced inflammatory cell infiltration and protected AE2 cell damage post-irradiation. The early delivery of UC-MSCs with SOD3 infection demonstrated better outcomes than UC-MSC treatment alone.

SOD3 reduces collagen levels ameliorated by US-MSCs in pulmonary

To determine if the combined cell and gene therapy of SOD3-infected UC-MSCs was able to reduce the characteristic collagen deposition in the lungs after irradiation, we performed a biochemical assay to test lung hydroxyproline (Hyp) content as a reliable marker of tissue collagen protein level. Consistent with the pathological results of Masson's trichrome staining, we found that the Hyp content in DS- and DU-treated animals was similar to the radiation-only animals (UI group) at 120 days post-radiation. In contrast, the Hyp content in ES- and EU-treated animals was significantly lower than that in radiation-only animals (UI group) at 120 days post-radiation. The Hyp content in ES-treated animals was significantly lower than that in EU-treated animals at 120 days post-irradiation (Figure 5A). These data manifested that the early delivery of UC-MSCs, but not the late delivery, reduced the accumulation of lung collagen protein. Furthermore, the early delivery of UC-MSCs with SOD3 infection achieved better results than UC-MSC treatment alone.

SOD3 restores redox state homeostasis ameliorated by US-MSCs in pulmonary

Because oxidative stress has been considered to trigger and sustain the pathogenesis of irradiation pulmonary fibrosis, we examined whether SOD3-infected UC-MSC treatment reduced oxidant stress as

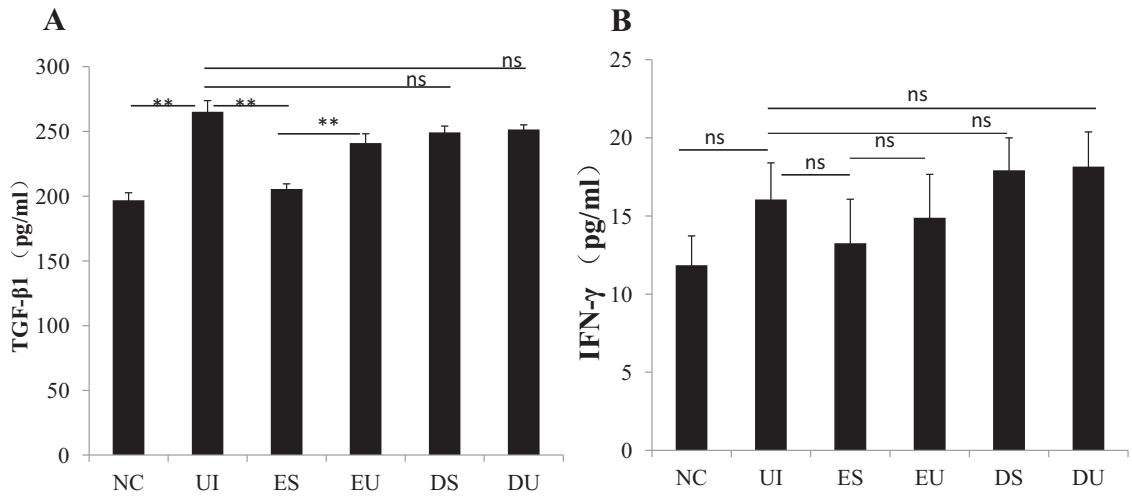

Figure 6. SOD3 improved the inflammation status ameliorated by US-MSCs in pulmonary. Lung samples were collected from animals at 120 days post-irradiation and were analyzed using ELISA (n = 6). Error bars represent the SEM. Single asterisk represents $P < 0.05$ and double asterisk indicates $P < 0.01$. Abbreviations: DS, delayed injection of SOD3 infected UC-MSCs; DU, delayed injection of UC-MSCs; ES, early injection of SOD3 infected UC-MSCs; EU, early injection of UC-MSCs; NC, normal control; n.s., not significant; UI, untreated irradiation.

determined by MDA content, and restored the antioxidant status *in vivo* as determined by enzymatic activities of total SOD and CAT.

The activities of total SOD and CAT in ES-treated animals were significantly higher than those in EU-treated animals at 120 days post-irradiation. The activities of total SOD and CAT in ES- and EU-treated animals were significantly higher than those in radiation-only animals at 120 days post-irradiation (Figure 5B and 5C). The activities of total SOD and CAT in DS- and DU-treated animals were similar as in radiation-only animals (UI group) at 120 days post-radiation (Figure 5B and 5C). The MDA content in DS- and DU-treated animals was similar as in radiation-only animals at 120 days post-irradiation. The MDA content in ES- and EU-treated animals was significantly lower than that in radiation-only animals (UI group) at 120 days post-irradiation. The MDA content in the ES-treated animals was significantly lower than that in EU-treated animals at 120 days post-irradiation (Figure 5D). These data indicated that the early delivery of UC-MSCs, but not the late delivery, prevented oxidative stress and increased antioxidant status in pulmonary. In addition, the early delivery of SOD3-infected UC-MSCs showed better results than UC-MSC treatment alone.

SOD3 improves the inflammation status ameliorated by US-MSCs in serum

As one of the key pro-fibrotic cytokines involved in the pathogenesis of pulmonary fibrosis, TGF-β1 is crucial in promoting proliferation of fibroblasts, driving differentiation of fibroblasts to myofibroblasts, increasing synthesis of extracellular matrix and stimulating protease inhibitor expression. IFN-γ, an anti-fibrotic cytokine, plays pivotal roles in modulating immune responses, inhibiting fibroblast proliferation and reducing extracellular matrix deposition [26]. We measured the levels of TGF-β1 and IFN-γ in serum using ELISA kits. Consistent with the previous reports, we found that the TGF-β1 levels in serum significantly increased at 120 days post-irradiation compared with normal control animals. The TGF-β1 levels in DS- and DU-treated animals were similar to the radiation-only animals (UI group) at 120 days post-radiation. The TGF-β1 levels in ES- and EU-treated animals were significantly lower than that in radiation-only animals (UI group) at 120 days post-radiation. The TGF-β1 level in the ES-treated animals was lower than that in the EU-treated animals at 120 days post-irradiation (Figure 6A).

However, there was no significant difference in the IFN-γ level among the six groups: NC, UI, DS, DU, ES and EU (Figure 6B). These data indicated the early delivery of UC-MSCs, but not the late delivery, reversed the imbalance of cytokine expression in serum. The early delivery of SOD3-infected UC-MSCs showed better results than UC-MSC treatment alone.

Discussion

In the present study, we demonstrated that in a mouse model of RPF that the early administration of UC-MSCs improved the lung histological damage, reduced collagen deposition, inhibited (myo)fibroblast proliferation, reduced inflammatory cell infiltration, protected

AE2 cells injury, prevented oxidative stress and increased antioxidant status and reduced pro-fibrotic TGF-β1 level in serum. Furthermore, the early treatment with SOD3-infected UC-MSCs resulted in further improvement. Our data reinforces the previous observation that the early delivery of MSCs, transduced or not to express protective mediators such as SOD3, lessened the occurrence of subsequent fibrosis development in a mice model of RPF. However, we failed to confirm our hypothesis that the therapeutic effects of UC-MSCs transduced to express SOD3 during established fibrosis.

Accumulated evidence supported that oxidative damage induced by irradiation dramatically contributed to the formation of RPF [2]. Hence, manipulation of own natural enzyme defense system against oxidative damage has been proposed and tested in recent years. Of this class of endogenous enzyme defense systems, SOD, the only enzymatic system decomposing superoxide radicals to H_2O_2, has received special attention for treating oxidative stress–related diseases, especially in the lung [27]. SOD-related treatment has shown to attenuate lung damage and improve survival in mice [26,28–33]. SOD3 is the only antioxidant enzyme in the ECM and extracellular space that is known to enzymatically scavenge superoxide radicals and thereby prevent the formation of many other reactive oxygen metabolites [21]. In the lung interstitium, SOD3 has been shown to be highly localized in areas containing high amounts of type I collagen fibers [19–22,27]. Low/absent SOD3 in fibrotic areas of human lungs with usual interstitial pneumonia (UIP) suggests that these regions may be susceptible to increased oxidant-mediated injury during disease progression. The re-expression of SOD3 in regenerative alveolar areas may represent an attempt to compensate for increased oxidant stress [34]. The distribution characteristic of SOD3 in the interstitial space suggests to us that SOD3 may demonstrate unique properties defended against oxidative damage induced-collagen deposition and final fibrosis. Therefore, exogenous SOD3 administration seems prospective for treatment of lung fibrosis.

Since administration of MSCs protective and restorable effects of damaged lung induced by bleomycin [9], irradiation [16] and LPS [17] have been shown. In addition, MSCs themselves have exerted antioxidative properties [35]. Human MSCs appears to be more feasible and safer than murine MSCs in the treatment for lung injury [13]. Based on these observations from previous reports, UC-MSCs were used to deliver SOD3 using an adenoviral gene transfer approach for overcoming short half-life of SODs and achieving selective and durable SOD3 release in the lung. Indeed, we found that RPF was greater mitigated with the early delivery of SOD3-infected UC-MSC treatment than UC-MSC treatment alone. We further examined whether the efficiency of SOD3 at later stage after irradiation (60 days post-irradiation) could modulate the microenvironment and finally attenuate fibrosis. Unfortunately, we did not observe any beneficial potential for irradiation-induced lung fibrosis by the late injection of UC-MSCs with or without SOD3 infection. This finding was consistent with the previous reports [5,16] that injection of MSCs at a later stage after irradiation would be involved in fibrosis development.

Notably, some UC-MSCs were detected in lung sections from UC-MSC–treated animals using immunohistochemical staining of a human nuclei marker, MAB1281. Reports [8,9,36] from the early period of MSC-based cell therapy for lung fibrosis demonstrated that injected MSCs could survive, engraft, even differentiate into typical AE2 cell phenotype and repair injured lung tissues. However, subsequently studies disclosed and supported that the level of engraftment of transplanted MSCs in host lungs of recipient animals was rare and very low [14,15,17,18,37–39]. The exact mechanisms of MSC actions in lung repair are poorly understood [10], but paracrine actions of MSCs have been highlighted that MSCs produce bioactive molecules and exert anti-scarring, anti-inflammatory and anti-apoptotic effects on target cells and surrounding inflammatory cells. The direct evidence of paracrine actions has been obtained and confirmed from lung [15], heart [40] and liver [41] injury animal models that conditioned medium (CM) generated from MSCs significantly reduced damage and stimulated regeneration *in vivo*. Down-regulation of pro-fibrotic cytokines and up-regulation of anti-fibrotic cytokines have been proposed as one of the paracrine actions of MSCs. TGF-β1 has long been considered as a typical pro-fibrotic cytokine in the pathogenesis of pulmonary fibrosis [42]. Up-regulation of the plasma levels of TGF-β1 in patients with idiopathic pulmonary fibrosis has been reported previously [43,44]. Most studies found that TGF-β1 levels in serum were increased in animal model of fibrosis [42]. Treatment of TGF-β1 antibodies significantly attenuated bleomycin-induced pulmonary fibrosis [45]. Our results demonstrated that the early delivery of UC-MSCs significantly reduced the level of TGF-β1 in serum. The additional effects of SOD3 on pro-fibrotic cytokine TGF-β1 may be derived from its own function of anti-oxidative damage.

IFN-γ, as a classical anti-fibrotic cytokine, can inhibit TGF-β1 expression, fibroblast proliferation, differentiation of fibroblasts to myofibroblasts (epithelial-mesenchymal transition, EMT) and collagen synthesis [46,47]. However, we did not detect any difference in the IFN-γ level among the six groups. The IFN-γ level in serum may compromise in the time course of

irradiation and return to the normal level. Further study is needed to determine the time course of IFN-γ level in serum using ELISA and other more precise methods, and to examine more types of cytokines and bioactive factors on systemic (serum) and local (lung tissue and bronchoalveolar lavage fluid) levels *in vivo*.

Stimulation of endogenous regeneration mechanisms have been suggested as one of the paracrine actions of MSCs, and was verified in animal models of lung fibrosis [15], liver injury [41], acute kidney failure [48] and stroke [49]. Our immunohistochemical results supported that the early administration of MSCs would significantly increase an AE2 cell marker SPB expression in lung sections. Furthermore, the early administration of MSCs demonstrated a more normalized distribution and abundance of AE2 cells in the alveolar walls in the parenchyma. This observation suggested that the early administration of MSCs stimulated AE2 cell regeneration and protected AE2 cells from free radical damage. This finding was consistent with the significant reductions of TGF-β1 levels in serum following the early administration of MSCs. The reductions of TGF-β1 levels in serum may extenuate the proliferation of fibroblast and EMT in the lung. We performed (myo)fibroblast marker α-SMA staining in lung sections and found that myofibroblast proliferation in the early delivery of UC-MSC–treated animals was significantly reduced, indicating the early UC-MSC treatment inhibited pulmonary fibrosis in part by inhibiting myofibroblast transformation and EMT. Exosomes derived from UC-MSCs could ameliorate carbon tetrachloride (CCl_4)-induced liver fibrosis by inhibiting EMT and protecting hepatocytes [50].

Over-expression of SOD3 in mice ameliorated acute radiation–induced injury through attenuation of the macrophage response and decreased TGF-β1 activation with a subsequent down-regulation of the profibrotic TGF-β pathway [51]. Consistent with this report, our data demonstrated that the macrophage infiltration in lung (as evidenced by Iba1 staining) was significantly reduced in the early administration of SOD3-infected UC-MSCs compared with UC-MSC treatment alone. In addition, SOD3 can also stabilize the ECM components by preventing reactive oxygen species (ROS)-induced degradation and further prevent TGF-β activation through ECM-stimulated mechanisms. Thus, modulation of TGF-β activity may be yet another mechanism in which SOD3 protects against pulmonary fibrosis [21].

Conclusions

In conclusion, we have shown that exogenous UC-MSC administration to RPF at the early stage significantly attenuated fibrosis through paracrine therapeutic effects of UC-MSCs. Furthermore, the therapeutic effects of UC-MSCs were largely strengthened by SOD3.

To our knowledge, this is the first study to determine the combined therapeutic effects of cell and gene therapy for RPF, and may provide pre-clinical data for treatment of RPF using human MSCs and SOD3.

Acknowledgments

This work was supported by grants from the National Natural Science Foundation of China (81670180, 8161101575, 81370077 and 81001220), Beijing Nova Program of Beijing Municipal Science and Technology Commission (Z171100001117091), Chongqing Science and Technology Committee (cstc2016jcyjA0030 and 2016cstc-jbky-01702), Chongqing Municipal Commission of Health and Family Planning (2016MSXM103), National Institute of Genetics (NIG) Collaborative Research Program (2016-A2-4). The funders had no role in study design, data collection and analysis, decision to publish or preparation of the manuscript.

Disclosure of interests: The authors have no commercial, proprietary or financial interest in the products or companies described in this article.

References

[1] Almeida C, Nagarajan D, Tian J, Leal SW, Wheeler K, Munley M, et al. The role of alveolar epithelium in radiation-induced lung injury. PLoS One 2013; 8(1):e53628. doi:10.1371/journal.pone.0053628.

[2] Williams JP, Johnston CJ, Finkelstein JN. Treatment for radiation-induced pulmonary late effects: spoiled for choice or looking in the wrong direction? Curr Drug Targets 2010;11(11):1386–94.

[3] Movsas B, Raffin TA, Epstein AH, Link CJ Jr. Pulmonary radiation injury. Chest 1997;111(4):1061–76.

[4] Nagarajan D, Melo T, Deng Z, Almeida C, Zhao W. ERK/GSK3β/Snail signaling mediates radiation-induced alveolar epithelial-to-mesenchymal transition. Free Radic Biol Med 2012;52(6):983–92. doi:10.1016/j.freeradbiomed.2011.11.024.

[5] Epperly MW, Guo H, Gretton JE, Greenberger JS. Bone marrow origin of myofibroblasts in irradiation pulmonary fibrosis. Am J Respir Cell Mol Biol 2003;29(2):213–24.

[6] Weiss DJ. Concise review: current status of stem cells and regenerative medicine in lung biology and diseases. Stem Cells 2014;32(1):16–25. doi:10.1002/stem.1506.

[7] Salem HK, Thiemermann C. Mesenchymal stromal cells: current understanding and clinical status. Stem Cells 2010;28(3):585–96. doi:10.1002/stem.269.

[8] Kotton DN, Ma BY, Cardoso WV, Sanderson EA, Summer RS, Williams MC, et al. Bone marrow-derived cells as progenitors of lung alveolar epithelium. Development 2001;128(24):5181–8.

[9] Ortiz LA, Dutreil M, Fattman C, Pandey AC, Torres G, Go K, et al. Interleukin 1 receptor antagonist mediates the antiinflammatory and antifibrotic effect of mesenchymal

stem cells during lung injury. Proc Natl Acad Sci USA 2007;104(26):11002–7.
[10] Abreu SC, Antunes MA, Pelosi P, Morales MM, Rocco PR. Mechanisms of cellular therapy in respiratory diseases. Intensive Care Med 2011;37(9):1421–31. doi:10.1007/s00134-011-2268-3.
[11] Tropea KA, Leder E, Aslam M, Lau AN, Raiser DM, Lee JH, et al. Bronchioalveolar stem cells increase after mesenchymal stromal cell treatment in a mouse model of bronchopulmonary dysplasia. Am J Physiol Lung Cell Mol Physiol 2012;302(9):L829–37. doi:10.1152/ajplung.00347.2011.
[12] Islam MN, Das SR, Emin MT, Wei M, Sun L, Westphalen K, et al. Mitochondrial transfer from bone-marrow-derived stromal cells to pulmonary alveoli protects against acute lung injury. Nat Med 2012;18(5):759–65. doi:10.1038/nm.2736.
[13] Aguilar S, Nye E, Chan J, Loebinger M, Spencer-Dene B, Fisk N, et al. Murine but not human mesenchymal stem cells generate osteosarcoma-like lesions in the lung. Stem Cells 2007;25(6):1586–94.
[14] Moodley Y, Atienza D, Manuelpillai U, Samuel CS, Tchongue J, Ilancheran S, et al. Human umbilical cord mesenchymal stem cells reduce fibrosis of bleomycin-induced lung injury. Am J Pathol 2009;175(1):303–13. doi:10.2353/ajpath.2009.080629.
[15] Cargnoni A, Ressel L, Rossi D, Poli A, Arienti D, Lombardi G, et al. Conditioned medium from amniotic mesenchymal tissue cells reduces progression of bleomycin-induced lung fibrosis. Cytotherapy 2012;14(2):153–61. doi:10.3109/14653249.2011.613930.
[16] Yan X, Liu Y, Han Q, Jia M, Liao L, Qi M, et al. Injured microenvironment directly guides the differentiation of engrafted Flk-1(+) mesenchymal stem cell in lung. Exp Hematol 2007;35(9):1466–75.
[17] Mei SH, McCarter SD, Deng Y, Parker CH, Liles WC, Stewart DJ. Prevention of LPS-induced acute lung injury in mice by mesenchymal stem cells overexpressing angiopoietin 1. PLoS Med 2007;4(9):e269.
[18] Aguilar S, Scotton CJ, McNulty K, Nye E, Stamp G, Laurent G, et al. Bone marrow stem cells expressing keratinocyte growth factor via an inducible lentivirus protects against bleomycin-induced pulmonary fibrosis. PLoS ONE 2009;4(11):e8013. doi:10.1371/journal.pone.0008013.
[19] Fattman CL, Tan RJ, Tobolewski JM, Oury TD. Increased sensitivity to asbestos-induced lung injury in mice lacking extracellular superoxide dismutase. Free Radic Biol Med 2006;40(4):601–7.
[20] Bowler RP, Nicks M, Warnick K, Crapo JD. Role of extracellular superoxide dismutase in bleomycin-induced pulmonary fibrosis. Am J Physiol Lung Cell Mol Physiol 2002;282(4):L719–26.
[21] Gao F, Kinnula VL, Myllärniemi M, Oury TD. Extracellular superoxide dismutase in pulmonary fibrosis. Antioxid Redox Signal 2008;10(2):343–54.
[22] Fattman CL, Chang LY, Termin TA, Petersen L, Enghild JJ, Oury TD. Enhanced bleomycin-induced pulmonary damage in mice lacking extracellular superoxide dismutase. Free Radic Biol Med 2003;35(7):763–71.
[23] Wei L, Zhang J, Xiao XB, Mai HX, Zheng K, Sun WL, et al. Multiple injections of human umbilical cord-derived mesenchymal stromal cells through the tail vein improve microcirculation and the microenvironment in a rat model of radiation myelopathy. J Transl Med 2014;12:246. doi:10.1186/s12967-014-0246-6.
[24] You H, Wei L, Zhang J, Wang JN. Vascular endothelial growth factor enhanced the angiogenesis response of human umbilical cord-derived mesenchymal stromal cells in a rat model of radiation myelopathy. Neurochem Res 2015;40(9):1892–903. doi:10.1007/s11064-015-1684-0.
[25] Wei L, Zhou Y, Liu CJ, Zheng K, You H. Demyelination occurred as the secondary damage following diffuse axonal loss in a rat model of radiation myelopathy. Neurochem Res 2017;doi:10.1007/s11064-016-2128-1.
[26] Mahmood J, Jelveh S, Zaidi A, Doctrow SR, Hill RP. Mitigation of radiation-induced lung injury with EUK-207 and genistein: effects in adolescent rats. Radiat Res 2013;179(2):125–34. doi:10.1667/RR2954.1.
[27] Kinnula VL, Crapo JD. Superoxide dismutases in the lung and human lung diseases. Am J Respir Crit Care Med 2003;167(12):1600–19.
[28] Epperly M, Bray J, Kraeger S, Zwacka R, Engelhardt J, Travis E, et al. Prevention of late effects of irradiation lung damage by manganese superoxide dismutase gene therapy. Gene Ther 1998;5(2):196–208.
[29] Epperly MW, Defilippi S, Sikora C, Gretton J, Kalend A, Greenberger JS. Intratracheal injection of manganese superoxide dismutase (MnSOD) plasmid/liposomes protects normal lung but not orthotopic tumors from irradiation. Gene Ther 2000;7(12):1011–18.
[30] Epperly MW, Travis EL, Sikora C, Greenberger JS. Manganese [correction of Magnesium] superoxide dismutase (MnSOD) plasmid/liposome pulmonary radioprotective gene therapy: modulation of irradiation-induced mRNA for IL-I, TNF-alpha, and TGF-beta correlates with delay of organizing alveolitis/fibrosis. Biol Blood Marrow Transplant 1999;5(4):204–14.
[31] Epperly MW, Epstein CJ, Travis EL, Greenberger JS. Decreased pulmonary radiation resistance of manganese superoxide dismutase (MnSOD)-deficient mice is corrected by human manganese superoxide dismutase-Plasmid/Liposome (SOD2-PL) intratracheal gene therapy. Radiat Res 2000;154(4):365–74.
[32] Epperly MW, Bray JA, Krager S, Berry LM, Gooding W, Engelhardt JF, et al. Intratracheal injection of adenovirus containing the human MnSOD transgene protects athymic nude mice from irradiation-induced organizing alveolitis. Int J Radiat Oncol Biol Phys 1999;43(1):169–81.
[33] Vujaskovic Z, Batinic-Haberle I, Rabbani ZN, Feng QF, Kang SK, Spasojevic I, et al. A small molecular weight catalytic metalloporphyrin antioxidant with superoxide dismutase (SOD) mimetic properties protects lungs from radiation-induced injury. Free Radic Biol Med 2002;33(6):857–63.
[34] Kinnula VL, Hodgson UA, Lakari EK, Tan RJ, Sormunen RT, Soini YM, et al. Extracellular superoxide dismutase has a highly specific localization in idiopathic pulmonary fibrosis/usual interstitial pneumonia. Histopathology 2006;49(1):66–74.
[35] Cho KA, Woo SY, Seoh JY, Han HS, Ryu KH. Mesenchymal stem cells restore CCl_4-induced liver injury by an antioxidative process. Cell Biol Int 2012;36(12):1267–74. doi:10.1042/CBI20110634.
[36] Yamada M, Kubo H, Kobayashi S, Ishizawa K, Numasaki M, Ueda S, et al. Bone marrow-derived progenitor cells are important for lung repair after lipopolysaccharide-induced lung injury. J Immunol 2004;172(2):1266–72.
[37] Cargnoni A, Gibelli L, Tosini A, Signoroni PB, Nassuato C, Arienti D, et al. Transplantation of allogeneic and xenogeneic placenta-derived cells reduces bleomycin-induced lung fibrosis. Cell Transplant 2009;18(4):405–22. doi:10.3727/096368909788809857.
[38] Rojas M, Xu J, Woods CR, Mora AL, Spears W, Roman J, et al. Bone marrow-derived mesenchymal stem cells in repair of the injured lung. Am J Respir Cell Mol Biol 2005;33(2):145–52.

[39] Liebler JM, Lutzko C, Banfalvi A, Senadheera D, Aghamohammadi N, Crandall ED, et al. Retention of human bone marrow-derived cells in murine lungs following bleomycin-induced lung injury. Am J Physiol Lung Cell Mol Physiol 2008;295(2):L285–92. doi:10.1152/ajplung.00222.2007.

[40] Timmers L, Lim SK, Arslan F, Armstrong JS, Hoefer IE, Doevendans PA, et al. Reduction of myocardial infarct size by human mesenchymal stem cell conditioned medium. Stem Cell Res 2007;1(2):129–37. doi:10.1016/j.scr.2008.02.002.

[41] van Poll D, Parekkadan B, Cho CH, Berthiaume F, Nahmias Y, Tilles AW, et al. Mesenchymal stem cell-derived molecules directly modulate hepatocellular death and regeneration *in vitro* and *in vivo*. Hepatology 2008;47(5):1634–43. doi:10.1002/hep.22236.

[42] Martin M, Lefaix J, Delanian S. TGF-beta1 and radiation fibrosis: a master switch and a specific therapeutic target? Int J Radiat Oncol Biol Phys 2000;47(2):277–90.

[43] Molina-Molina M, Lario S, Luburich P, Ramírez J, Carrión MT, Xaubet A. Quantifying plasma levels of transforming growth factor beta1 in idiopathic pulmonary fibrosis. Arch Bronconeumol 2006;42(8):380–3.

[44] Yong SJ, Adlakha A, Limper AH. Circulating transforming growth factor-beta (1): a potential marker of disease activity during idiopathic pulmonary fibrosis. Chest 2001;120(1 Suppl.):68S–70S.

[45] Nakao A, Fujii M, Matsumura R, Kumano K, Saito Y, Miyazono K, et al. Transient gene transfer and expression of Smad7 prevents bleomycin-induced lung fibrosis in mice. J Clin Invest 1999;104(1):5–11.

[46] Alhamad EH, Cal JG, Shakoor Z, Almogren A, AlBoukai AA. Cytokine gene polymorphisms and serum cytokine levels in patients with idiopathic pulmonary fibrosis. BMC Med Genet 2013;14:66. doi:10.1186/1471-2350-14-66.

[47] Ji Y, Wang T, Wei ZF, Lu GX, Jiang SD, Xia YF, et al. Paeoniflorin, the main active constituent of Paeonia lactiflora roots, attenuates bleomycin-induced pulmonary fibrosis in mice by suppressing the synthesis of type I collagen. J Ethnopharmacol 2013;149(3):825–32. doi:10.1016/j.jep.2013.08.017.

[48] Tögel F, Hu Z, Weiss K, Isaac J, Lange C, Westenfelder C. Administered mesenchymal stem cells protect against ischemic acute renal failure through differentiation-independent mechanisms. Am J Physiol Renal Physiol 2005;289(1):F31–42.

[49] Seyfried D, Ding J, Han Y, Li Y, Chen J, Chopp M. Effects of intravenous administration of human bone marrow stromal cells after intracerebral hemorrhage in rats. J Neurosurg 2006;104:313–18.

[50] Li T, Yan Y, Wang B, Qian H, Zhang X, Shen L, et al. Exosomes derived from human umbilical cord mesenchymal stem cells alleviate liver fibrosis. Stem Cells Dev 2013;22(6):845–54. doi:10.1089/scd.2012.0395.

[51] Rabbani ZN, Anscher MS, Folz RJ, Archer E, Huang H, Chen L, et al. Overexpression of extracellular superoxide dismutase reduces acute radiation induced lung toxicity. BMC Cancer 2005;5:59.